OFFICE OF NAVAL RESEARCH

Research Contract N00014-90-J-1178

R&T Code 413r008---001



Principal Investigator: **R. Stanley Williams**
Organization: **Regents of the University of California**

**TECHNICAL REPORT No. 9**

# SOLID-PHASE EQUILIBRIA FOR METAL-SILICON-OXYGEN TERNARY SYSTEMS: II: Sc, Y, AND La

by

**Haojie Yuan and R. Stanley Williams**

*Prepared for*

*Chemical Materials*



**University of California, Los Angeles**
Department of Chemistry & Biochemistry and Solid State Sciences Center
Los Angeles, CA 90024-1569

February, 1991

UNCLASSIFIED

SECURITY CLASSIFICATION OF THIS PAGE

# REPORT DOCUMENTATION PAGE

| | |
|---|---|
| 1a REPORT SECURITY CLASSIFICATION<br>UNCLASSIFIED | 1b RESTRICTIVE MARKINGS<br>N/A |
| 2a SECURITY CLASSIFICATION AUTHORITY<br>N/A | 3 DISTRIBUTION / AVAILABILITY OF REPORT<br>Approved for public release; distribution unlimited |
| 2b DECLASSIFICATION / DOWNGRADING SCHEDULE<br>N/A | |
| 4 PERFORMING ORGANIZATION REPORT NUMBER(S)<br>N/A | 5 MONITORING ORGANIZATION REPORT NUMBER(S) |
| 6a NAME OF PERFORMING ORGANIZATION<br>The Regents of the University of California<br>6b OFFICE SYMBOL (If applicable) | 7a NAME OF MONITORING ORGANIZATION<br>1) ONR Pasadena - Administrative<br>2) ONR Alexandria - Technical |
| 6c ADDRESS (City, State, and ZIP Code)<br>Office of Contracts & Grants Administration<br>U C L A, 405 Hilgard Avenue<br>Los Angeles, CA 90024 | 7b ADDRESS (City, State, and ZIP Code)<br>1) 1030 E. Green Street, Pasadena, CA 91106<br>2) 800 N. Quincy St., Arlington, VA 22217-500 |
| 8a NAME OF FUNDING / SPONSORING ORGANIZATION<br>Office of Naval Research<br>8b OFFICE SYMBOL (If applicable)<br>ONR | 9 PROCUREMENT INSTRUMENT IDENTIFICATION NUMBER<br>N00014-90-J-1178 |
| 8c ADDRESS (City, State, and ZIP Code)<br>800 N. Quincy Street, 614A:DHP<br>Arlington, VA 22217-5000 | 10 SOURCE OF FUNDING NUMBERS<br>PROGRAM ELEMENT NO. / PROJECT NO / TASK NO / WORK UNIT ACCESSION NO |

11 TITLE (Include Security Classification)
UNCLASSIFIED: SOLID-PHASE EQUILIBRIA FOR METAL-SILICON-OXYGEN TERNARY SYSTEMS: II: Sc, Y, AND La

12 PERSONAL AUTHOR(S) Haojie Yuan and R. Stanley Williams

| 13a TYPE OF REPORT | 13b TIME COVERED | 14 DATE OF REPORT (Year, Month, Day) | 15 PAGE COUNT |
|---|---|---|---|
| Tech.Rpt. #9 | FROM June'90 TO Feb'91 | 28 Feb 91 | 11 pp 6 Figs |

16 SUPPLEMENTARY NOTATION

| 17 COSATI CODES | | | 18 SUBJECT TERMS (Continue on reverse if necessary and identify by block number) |
|---|---|---|---|
| FIELD | GROUP | SUB-GROUP | ternary phase diagrams - thermodynamics - phase stability - Y-Si-O - La-Si-O - three-element systems -metal oxides - high-$T_c$ superconductors - interfacial chemistry |
| | | | |
| | | | |

19 ABSTRACT (Continue on reverse if necessary and identify by block number)

We have derived ternary-phase diagrams of the type M-Si-O, where M=Sc, Y and La under the conditions of 298K and 1 atm oxygen partial pressure. These phase diagrams provide a direct view of the thermodynamics that governs stabilities of phases containing these elements in contact with each other, and should be useful for integrating Y- and La-based oxide superconductors with Si.

| 20 DISTRIBUTION / AVAILABILITY OF ABSTRACT | 21 ABSTRACT SECURITY CLASSIFICATION | |
|---|---|---|
| ☒ UNCLASSIFIED/UNLIMITED ☐ SAME AS RPT ☐ DTIC USERS | UNCLASSIFIED | |
| 22a NAME OF RESPONSIBLE INDIVIDUAL<br>R. Stanley Williams | 22b TELEPHONE (Include Area Code)<br>(213) 825-8818 | 22c OFFICE SYMBOL<br>UCLA |

DD FORM 1473, 84 MAR 83 APR edition may be used until exhausted. All other editions are obsolete.

SECURITY CLASSIFICATION OF THIS PAGE
UNCLASSIFIED

# Solid phase equilibria for metal-silicon-oxygen ternary systems II: Sc, Y and La

Haojie Yuan and R. Stanley Williams

Department of Chemistry and Biochemistry and
Solid State Science Center
University of California Los Angeles
Los Angeles, CA 90024-1569

## Abstract

We have derived ternary phase diagrams of the type M-Si-O, where M=Sc, Y and La under the conditions of 298K and 1atm oxygen partial pressure. These phase diagrams provide a direct view of the thermodynamics that governs stabilities of phases containing these elements in contact with each other, and should be useful for integrating Y- and La-based oxide superconductors with Si.

## I. Introduction

The application of ternary phase diagrams to research on thin film structures has been recognized by many investigators.[1-6] A ternary phase diagram provides a direct view of the thermodynamics that govern the stability of the phases in contact with each other in a particular three-element system. Although such phase diagrams are strictly valid only for closed bulk systems, they are very helpful

in explaining the experimental results on the stabilities of thin film structures and in predicting the reactions that occur at interfaces between different materials.

In this work, phase diagrams for systems of the type M-Si-O, where M = Sc, Y and La, have been derived. These phase diagrams are important for understanding how the metal oxides ($Sc_2O_3$, $Y_2O_3$ and $La_2O_3$) and various high $T_C$ superconductors interact with elemental Si, $SiO_2$ and corresponding metal silicates, how silicates interact with elemental Si, and how the metals (Sc, Y and La) interact with $SiO_2$. This work extends a previous examination of M-Si-O systems, where M=Mg, Ca, Sr and Ba.[7] We will describe how the phase diagrams were determined, present the ternary diagrams for the M-Si-O systems, and discuss the use of these phase diagrams for understanding interfacial chemistry.

## II. Ternary Phase Diagram Determination

Ternary phase diagrams can be determined from calculations if the Gibbs energy data of all the relevant compounds are known or by performing phase stability experiments if the thermochemical data are unavailable[1,5] Since the Gibbs energy data for many phases in the Sc-Si-O, Y-Si-O and La-Si-O systems could not be found, we had to determine the phase diagrams for these systems by performing experiments.

We consulted the literature[8-17] to determine what phases exist in each system, and constructed the binary boundaries of the ternary diagrams. In addition, all three systems have silicates that require

the existence of tie-line segments between $M_2O_3$ and $SiO_2$. In the Sc-Si-O system, if a tie line connecting $Sc_2O_3$ and Si exists, then we can immediately determine all other tie lines in this system on the basis of Gibbs phase rule,[8] i.e. no two tie-lines can cross. Thus, we selected a mixture of $Sc_2O_3$ and Si with relative amounts of each corresponding to the following stoichiometric reaction:

$$6Sc_2O_3 + 29Si \Rightarrow 9SiO_2 + 4Sc_3Si_5.$$

This composition corresponds to the point where the potential $Sc_2O_3$-Si tie line intersects a different possibility, a $SiO_2$-$Sc_3Si_5$ tie line.

We mixed a small amount of 99.9% pure $Sc_2O_3$ and 99.8% pure Si powders, sealed the mixture in a small vacuum ampoule, and heated to the temperature of 800°C for 7 days to initiate any reaction. Samples of the mixture *before* and *after* heating were analyzed by the x-ray powder diffraction method to see what phases were present in the mixture, and the results are shown in Fig. 1. The two x-ray powder diffraction patterns are nearly the same. Therefore, no new phases were produced by heating, and we deduce that $Sc_2O_3$ and Si form a stable pseudobinary system. There should be a tie line connecting $Sc_2O_3$ and Si, and all other tie lines in the system are dictated by the Gibbs phase rule.

The same type of experiments were performed for the Y-Si-O and La-Si-O systems, except that the reaction mixtures chosen for these two systems were consistent with:

$$2Y_2O_3 + 11Si \Rightarrow 3SiO_2 + 4YSi_2 \text{ and}$$

$$2La_2O_3 + 11Si \Rightarrow 3SiO_2 + 4LaSi_2,$$

respectively. The x-ray powder diffraction patterns before and after heating for these two samples are presented in Figs. 2 and 3. We can see from the diffraction patterns that no new phases were produced in these two systems, although the relative intensities of some of the peaks did change. These changes are too small to be caused by phases transformations in the mixtures, and are most likely the result of physical changes in the powders. Thus, Si forms pseudobinary systems with both $Y_2O_3$ and $La_2O_3$, and the diagrams for these systems are also completely determined. The resulting phase diagrams for the Sc-Si-O, Y-Si-O and La-Si-O systems are presented in Figs. 4-6, respectively.

During the experiments, we found $La_2O_3$ is very air sensitive. It reacts readily with $H_2O$ and $CO_2$ to form hydroxides and carbonates. We collected x-ray powder diffraction patterns of both $La_2O_3$ powder taken directly from the reagent bottle and $La_2O_3$ powder that had been exposed to the air for two days, and then we compared both patterns with the pattern that we collected for Si and $La_2O_3$ mixed powders. Because the reaction of $La_2O_3$ powder with air is fairly rapid (after only two and half hours, a noticeable volume change of the $La_2O_3$ powder occurs), the x-ray powder pattern must be collected quickly. The scan times used for this study were 60 minutes long. The peak labeled Z in Fig. 3 is the result of phases formed by reactions of $La_2O_3$ with air. During the experiments, we also mixed $La_2O_3$ powder that had been exposed to the air for two days with Si powder, sealed a small amount of the mixture in a small vacuum ampoule and heated to 800°C. This led to an explosion of the ampoule. We deduce that this is because that $La_2O_3$ had

already absorbed $H_2O$ and $CO_2$ in the air to form hydroxides and carbonate. These compounds decomposed upon heating and the release of gases at the high temperature caused the explosion.

## III. Discussion

The phase diagrams for Sc-Si-O, Y-Si-O and La-Si-O are very similar. The only differences are the stoichiometries and number of the silicide phases and the number of silicates. These diagrams are quite different from some of those for the column II[7] and column IV[4,17] metal-silicon-oxygen phase diagrams. In the column II metal-silicon-oxygen systems,[7] the phase diagram for the Mg-Si-O system is very similar to the phase diagrams derived in this work, but the phase diagrams for the Ca-Si-O, Sr-Si-O and Ba-Si-O systems are more complicated. Compared to the phase diagrams present in this paper, there are more oxides and silicates in the Ca-Si-O, Sr-Si-O and Ba-Si-O systems. The oxides of Ca, Sr and Ba are reduced by Si, while $Sc_2O_3$, $Y_2O_3$ and $La_2O_3$ are stable in contact with Si. The phase diagram for Ti-Si-O system[4] is quite different from the phase diagrams derived here. There are more oxides in the Ti-Si-O system that are not stable in contact with Si, no Ti silicate exists and there are more silicides.

From the phase diagrams, we can see that the metal oxides ($Sc_2O_3$, $Y_2O_3$ and $La_2O_3$) are connected to silicon by tie lines. Thus, thin films of these oxides should be stable on silicon substrates. This information is potentially useful when considering the deposition of Y- and La- based superconductors on Si substrates.

Also, we can see that the oxides are stable in contact with the various metal silicides. Metal oxides react with silica to produce metal silicates, and thin films of these silicates should be stable if deposited on silicon substrates. One may think of using Y silicates or La silicates as interlayer materials between YBCO superconducting films and a silicon substrate, since ternary oxide compounds of this kind are very stable.[7] However, the lattice constants of the Y and La silicates[16] are very different from those of YBCO and Si, which most likely precludes being able to grow epitaxial structures. Sc, Y and La can all reduce $SiO_2$ to metal oxides and metal silicides, which means that from the thermodynamic point of view, these metals cannot be stable on $SiO_2$ substrates.

We can use the phase diagrams we derived to make the following estimations. Taking Sc-Si-O as an example from the diagram, for the $Sc_2SiO_5$-Sc and $Sc_2O_3$-Si tie lines to be true, we have:

$$\Delta G(Sc_2SiO_5) < \Delta G(Sc_2O_3) + \Delta G(SiO_2) \text{ and} \quad (1)$$

$$5\Delta G(Sc_2O_3) < 3\Delta G(Sc_2SiO_5). \quad (2)$$

By combining (2) with (1), we have:

$$\Delta G(Sc_2O_3) < 3/2\Delta G(SiO_2), \quad (3)$$

which puts an upper bound on the Gibbs energy of formation of $Sc_2O_3$. For $Sc_2Si_2O_7$, the same type of estimation also leads to the inequality in (3). The same estimates can be made in the Y-Si-O and La-Si-O systems also, and we derived the formulae corresponding to (3). The Gibbs energy data for the metal oxides and silicon dioxide are tabulated in Table I. The relations derived from the estimates made above are consistent with the literature data that exists.

Thus, the phase diagrams are consistent with the known thermochemical data for these systems.

## IV. Summary

Ternary phase diagrams have been derived for the metal (Sc, Y and La)-Si-O systems. These phase diagrams can be used as guides to understand the chemistry at the interfaces of different solids involving the represented elements. They can be determined from very simple experiments, but they can provide a great deal of insight into chemical reactivity at interfaces and designing new structures based on joining unlike materials at an interface.

## Acknowledgement

This work was supported in part by the Office of Naval Research. R. S. Williams received partial support from the Camille and Henry Dreyfus Foundation.

## Reference


1. G. P. Schwartz, G. J. Gaultieri, J. E. Griffith, C. D. Thurmond and B. Schwartz, J. Electrochem. Soc. **127**, 2488 (1980).
2. C. D. Thurmond, G. P. Schwartz, G. W. Kammlott and B. Schwartz, J. Electrochem. Soc. **127**, 1366 (1980).
3. G. P. Schwartz, Thin Solid Film **103**, 3 (1983).
4. R. Beyers, Mat. Res. Soc. Proc. **47**, 143 (1985).
5. C. T. Tsai and R. S. Williams, J. Mater. Res. **1**, 352 (1986).
6. J. H. Pugh and R. S. Williams, J. Mater. Res. **1**, 343 (1986).
7. H. Yuan and R. S. Williams, submitted for publication.
8. O. Kubaschewski and C. B. Alock, Metallurgical Thermochemistry, 5th edition (Pergamon Press, Oxford, New York,1979).
9. CRC Handbook of Chemistry and Physics, 68th edition (CRC press Inc. Boca Raton, Florida, 1987-1988).
10. A. S. Berezhnoi, Silicon and Its Binary System (Consultants Bureau, New York, 1979).
11. D. D. Wagman, W. H. Evens, V. B. Parker, R. H. Schumm, I. Halow, S. M. Bailey, K. I. Churney and R. L. Nuttall, J. of Physical and Chemical Reference Data **11**, Supplement No. 2 (1982).
12. N. A. Toropov, V. P. Barzakovskii, V. V. Lapin and N. N. Kurtseva, Handbook of Phase Diagrams of Silicate Systems, **1** and **2** (Israel Program for Scientific Translations, Jerusalem 1972).
13. M. Hansen, Constitution of Binary Alloys (McGraw-Hill, New York, 1969).

14. F. A. Shunk, Constitution of Binary Alloys, Second Supplement (McGraw-Hill, New York, 1969).

15. W. G. Moffatt, Binary Phase Diagrams Handbook (General Electric Co., Schenectady, 1977).

16. JCPDS Powder Diffraction File, Inorganic Phases, Alphabetical Index (Chemical and Mineral Name, 1987).

17. K. -H. Hellwege and O. Madelung, Landolt-Bornstein Numerical Data and Functional Relations in Science and Technology, New Series, III/7d1α (Springer-Verlag Berlin-Heidelberg, 1985).

Table I. Gibbs Energy Data for the Metal Oxides and $SiO_2$.[11]

| | $\Delta G$ ($M_2O_3$) (kJ/mol) | $3/2\Delta G(SiO_2)$ (kJ/mol) |
|---|---|---|
| $Sc_2O_3$ | -1819.36 | -1285.0 |
| $Y_2O_3$ | -1816.60 | -1285.0 |
| $La_2O_3$ | -1705.8 | -1285.0 |

## Figure Captions

Fig. 1. X-ray powder diffraction pattern for the powdered mixture of $Sc_2O_3$ and Si. (A) After heating at 800°C for 7 days, (B) before heating. X stands for $Sc_2O_3$.

Fig. 2. X-ray powder diffraction pattern for the powdered mixture of $Y_2O_3$ and Si. (A) After heating at 800°C for 7 days, (B) before heating. X stands for $Y_2O_3$.

Fig. 3. X-ray powder diffraction pattern for the powdered mixture of $La_2O_3$ and Si. (A) After heating at 800°C for 7 days, (B) before heating. X stands for $La_2O_3$. Z is due to the phase(s) caused by exposing the $La_2O_3$ powder to the air while the diffraction pattern was being collected.

Fig. 4. Sc-Si-O phase diagram at 298K and 1atm.

Fig. 5. Y-Si-O phase diagram at 298K and 1atm. Compounds from left to right on the $Y_2O_3$-$SiO_2$ tie-line are $Y_2SiO_5$, $Y_{14}Si_9O_{39}$, $Y_4Si_3O_{12}$ and $Y_2Si_2O_7$. $Y_{14}Si_9O_{39}$ and $Y_4Si_3O_{12}$ are indicated with the same point on the diagram because their compositions are nearly indistinguishable.

Fig. 6. La-Si-O phase diagram at 298K and 1atm. Compounds from left to right on the $La_2O_3$-$SiO_2$ tie-line are $La_2SiO_5$, $La_{14}Si_9O_{39}$, $La_4Si_3O_{12}$ and $La_2Si_2O_7$. $La_{14}Si_9O_{39}$ and $La_4Si_3O_{12}$ are indicated with the same point on the diagram because their compositions are nearly indistinguishable.

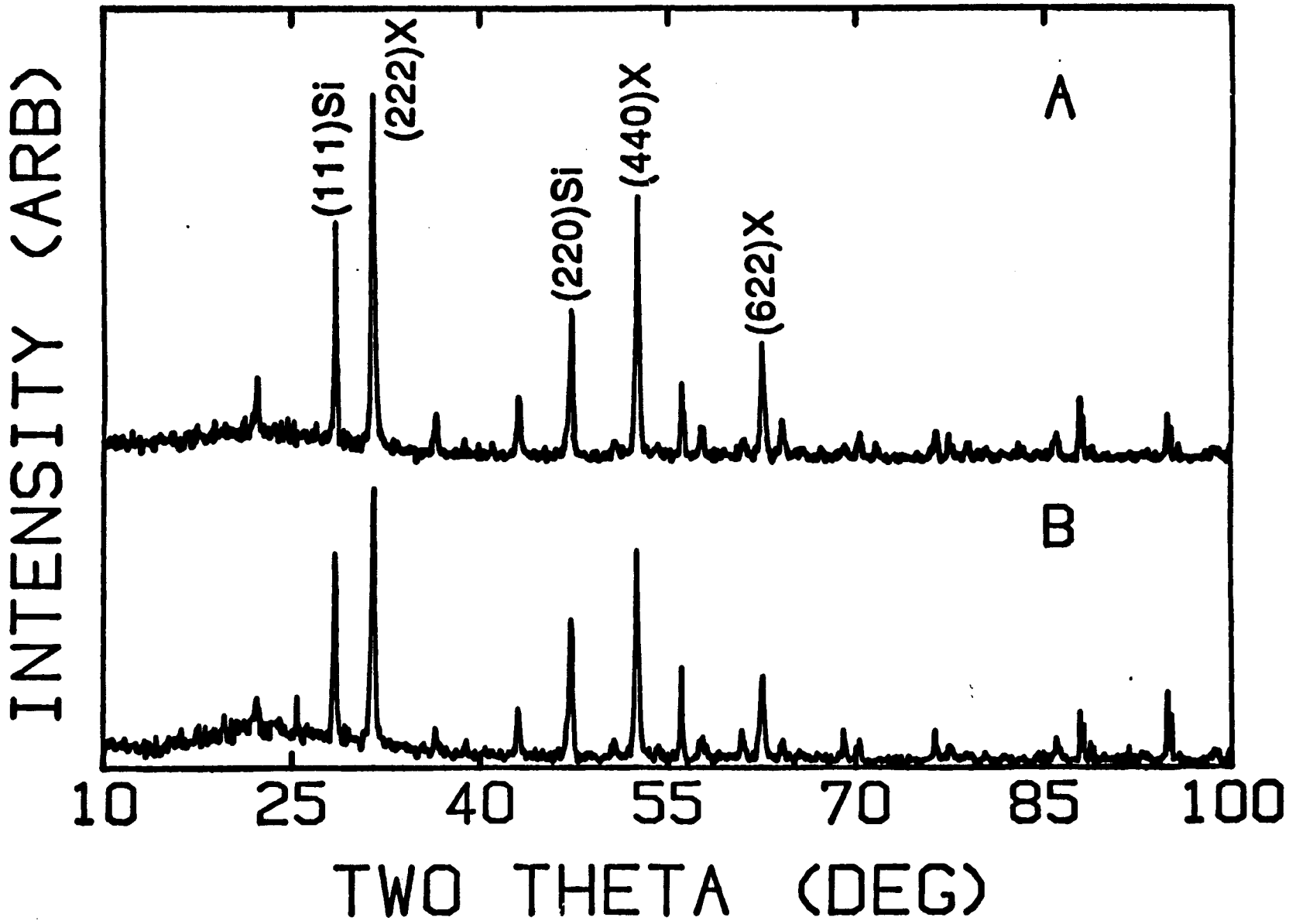
INTENSITY (ARB)
(111)Si
(222)X
(220)Si
(440)X
(622)X
A
B
10
25
40
55
70
85
100
TWO THETA (DEG)

Fig. 1

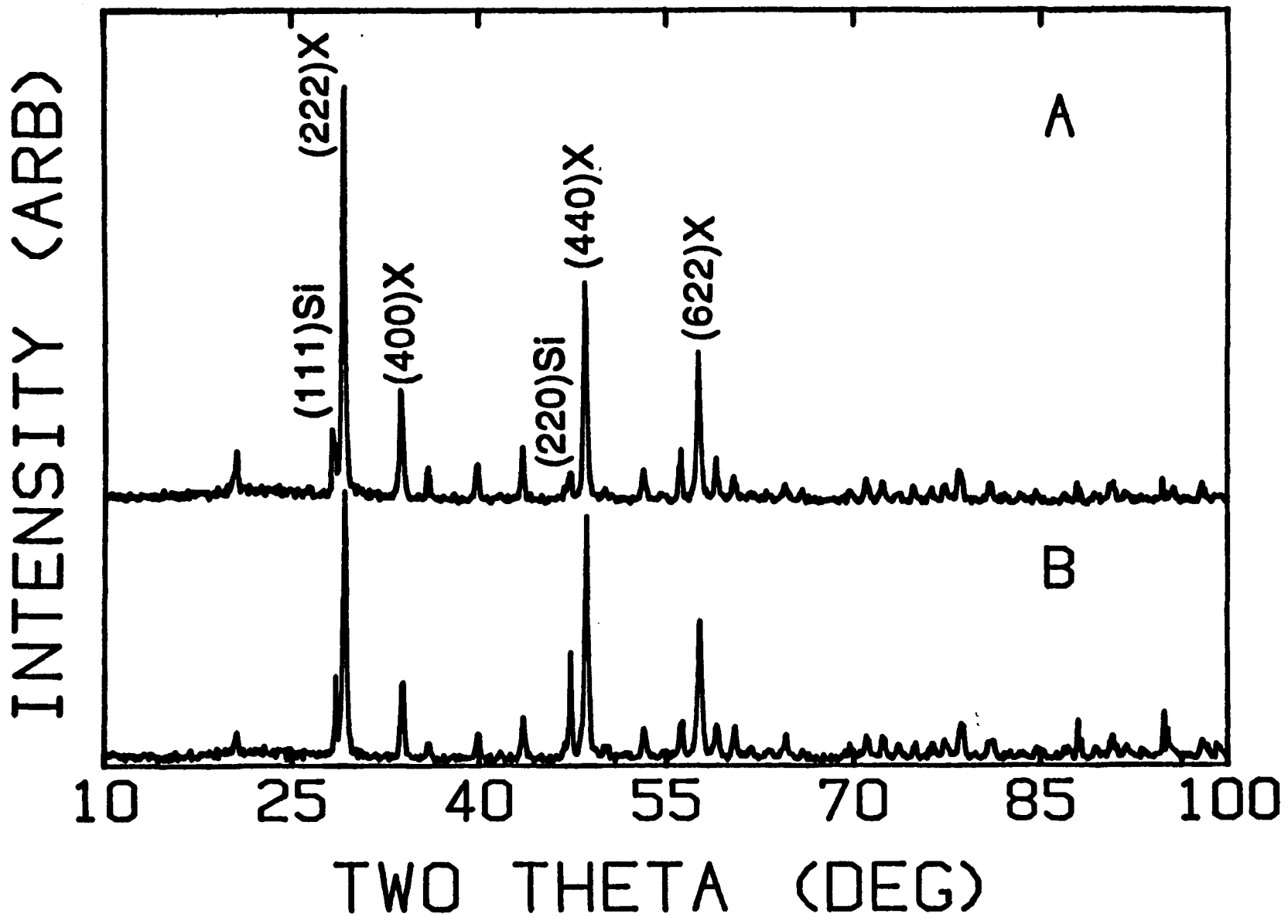
INTENSITY (ARB)
(111)Si
(222)X
(400)X
(220)Si
(440)X
(622)X
A
B
10
25
40
55
70
85
100
TWO THETA (DEG)

Fig. 2

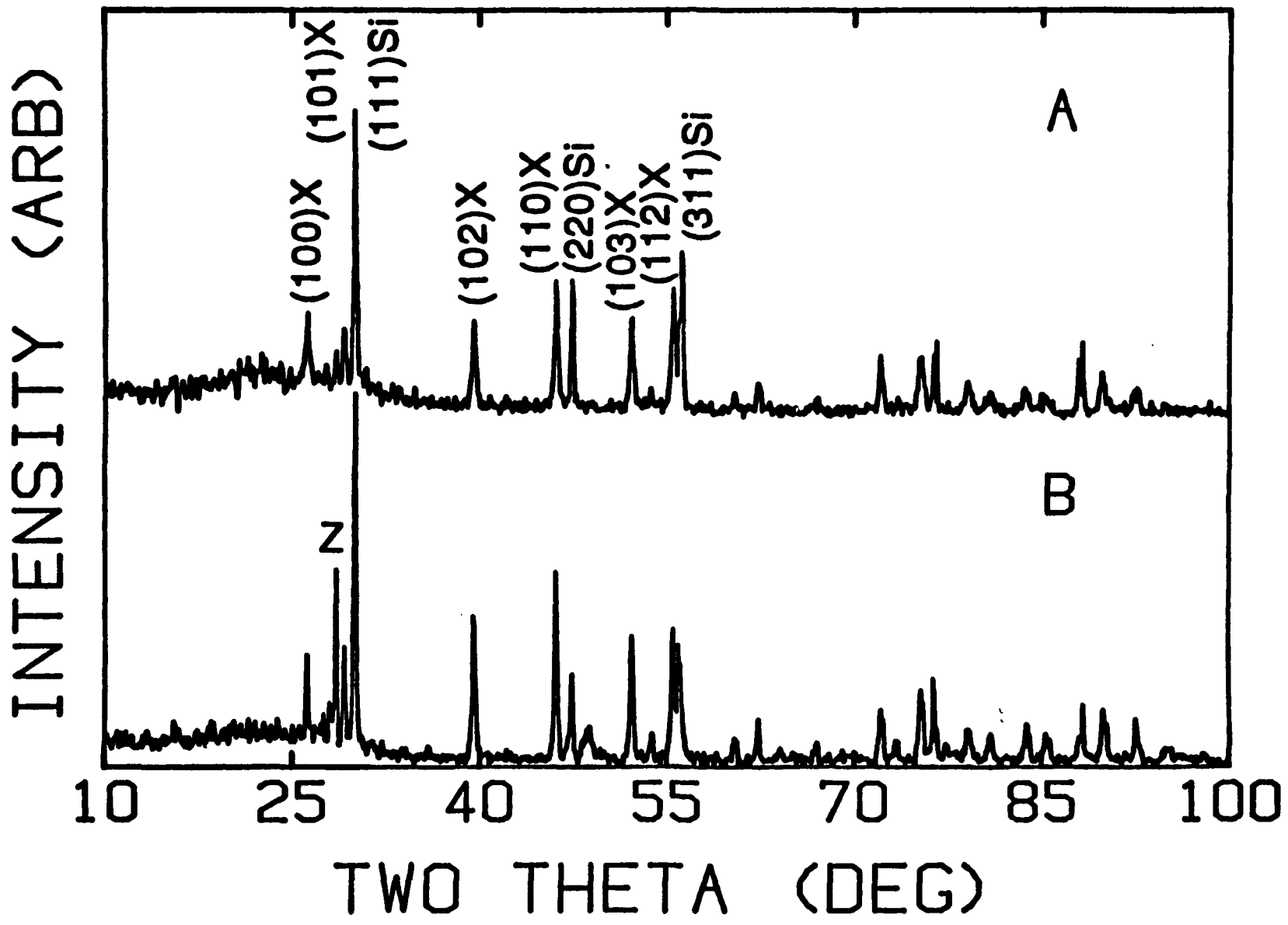
INTENSITY (ARB)
(100)X
(101)X
(111)Si
(102)X
(110)X
(220)Si
(103)X
(112)X
(311)Si
A
B
Z
10
25
40
55
70
85
100
TWO THETA (DEG)

Fig. 3

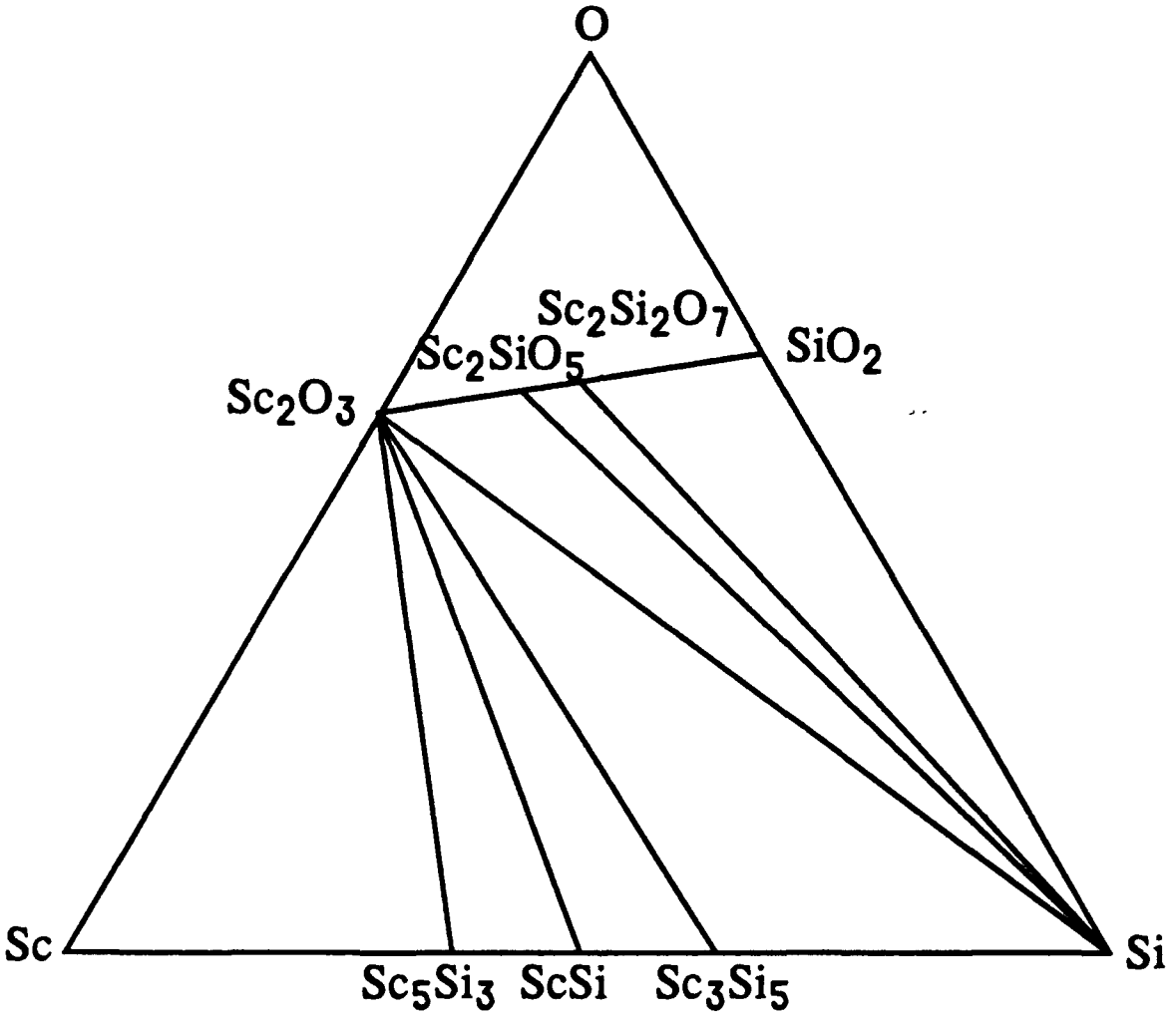


Fig. 4

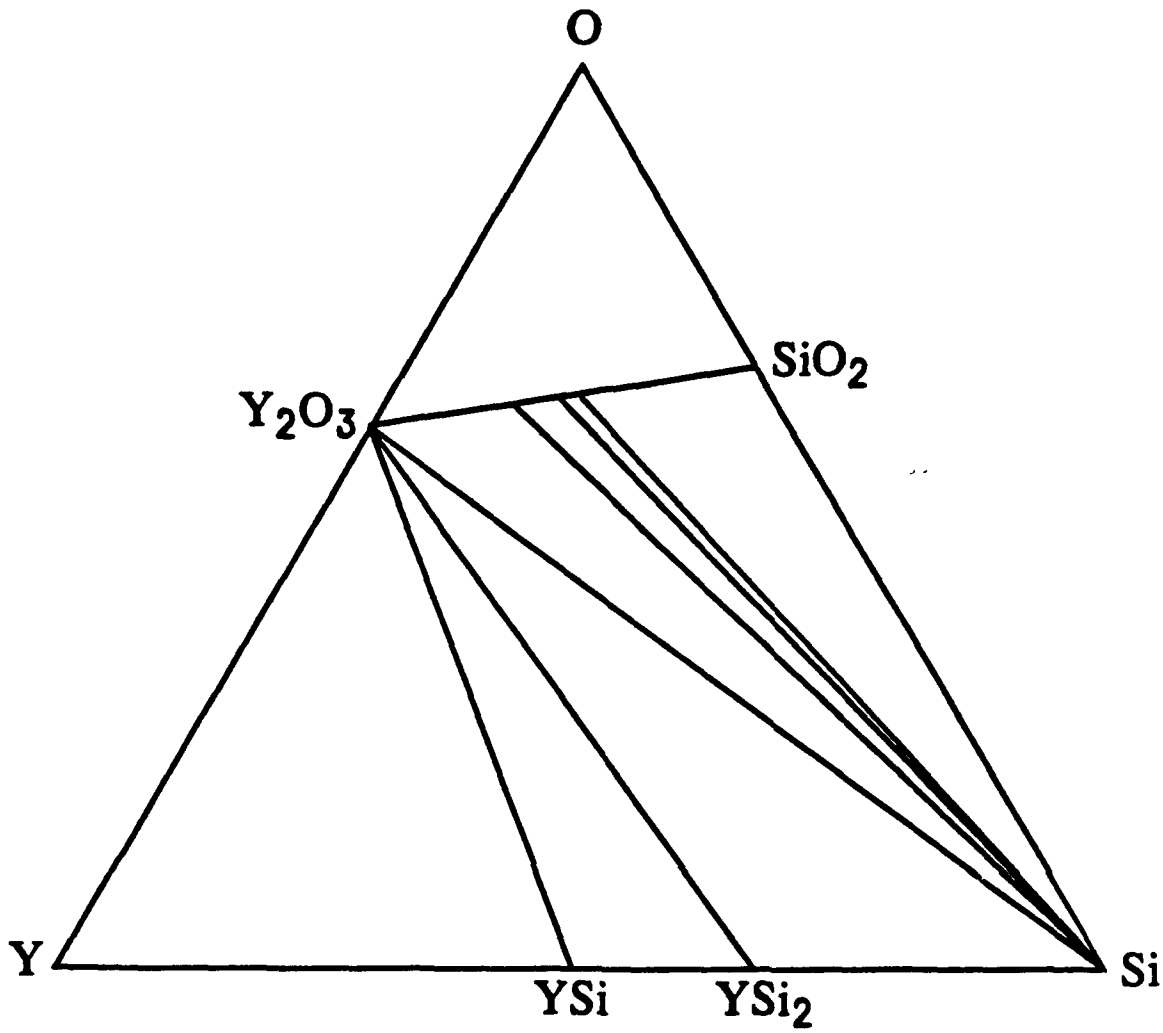


Fig. 5

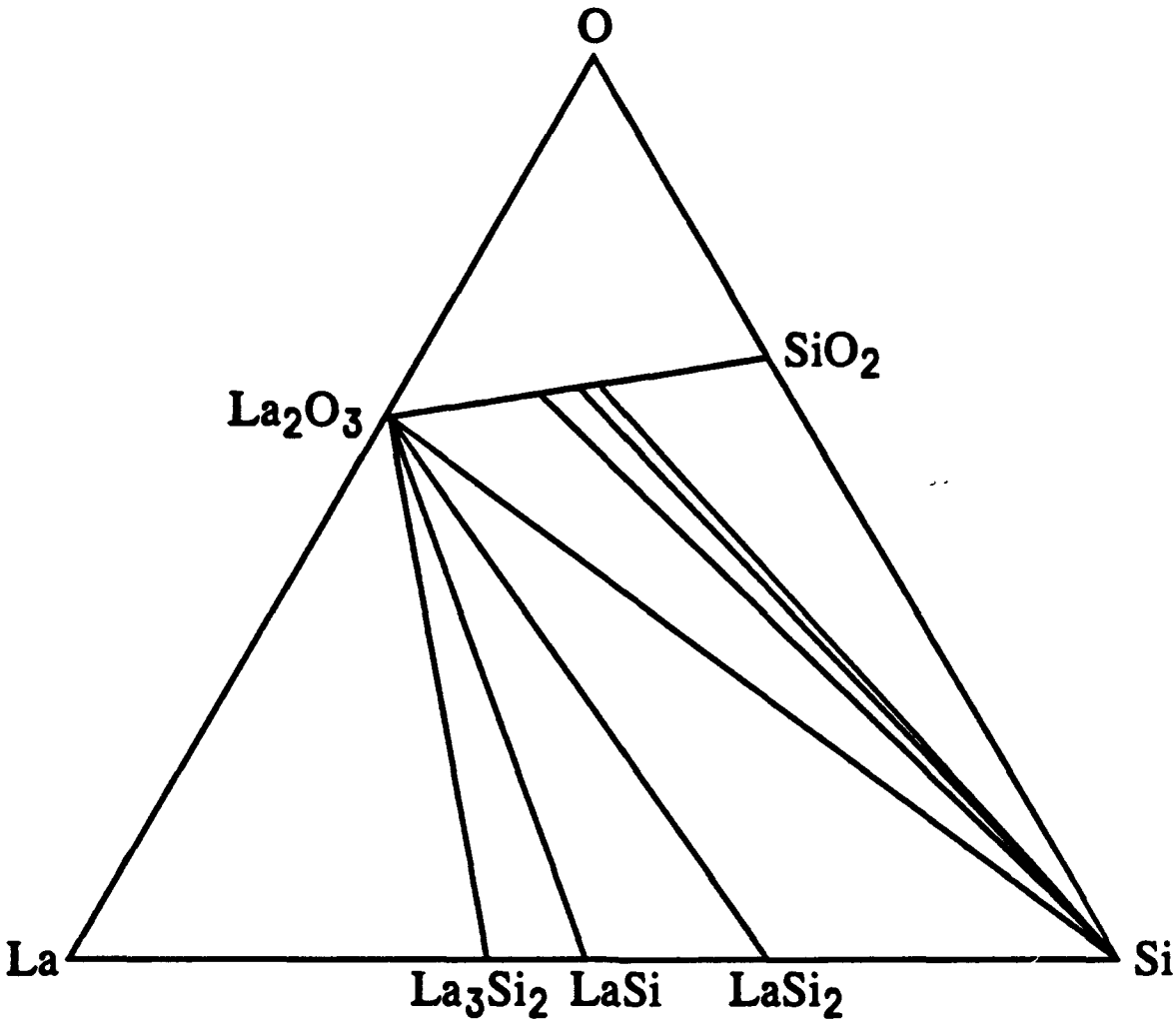


Fig. 6